J. theor. Biol. (2000) **204,** 505–519
doi:10.1006/jtbi.2000.2034, available online at http://www.idealibrary.com on IDEAL®

Modeling Complex Neutrophil Dynamics in the Grey Collie

CAROLINE HAURIE*, DAVID C. DALE†, RYSZARD RUDNICKI‡ AND MICHAEL C. MACKEY§‖

*Department of Physiology, Centre for Nonlinear Dynamics, McGill University, Canada
†Division of Hematology, Department of Medicine, University of Washington, U.S.A.
‡Institute of Mathematics, Polish Academy of Sciences, Staromiejska 8, 40-013 Katowice, Poland and
§Departments of Physiology, Physics, & Mathematics, Centre for Nonlinear Dynamics, McGill University, Canada

(*Received on* 3 *September* 1999, *Accepted in revised form on* 1 *March* 2000)

We have developed a mathematical model for the peripheral regulation of neutrophil production mediated by granulocyte colony-stimulating factor. We have used that model to show that the pattern of neutrophil oscillations in nine grey collies is consistent with the hypothesis that cyclical neutropenia is due to an oscillatory stem cell input to the neutrophil regulatory system, and not due to autonomous oscillations in the peripheral neutrophil regulatory system. In the process of interfacing our model with the laboratory data, we have estimated parameters for the peripheral neutrophil control system consistent with higher than normal apoptotic cell loss within the recognizable neutrophil precursors. This is in agreement with other experimental data. Our estimated model parameters also predict that the peripheral neutrophil production system is globally stable in the grey collies we studied. This further supports our hypothesis that the origin of the oscillatory behavior in cyclical neutropenia is in the stem cell population, consistent with other clinical and experimental evidence.

1. Introduction

Some hematological diseases display a distinct periodic nature in which one or more circulating cell types (white blood cells, red blood cells, platelets) oscillate with periods ranging from days to months (cf. Haurie *et al.* (1998) for a recent review). Of these periodic hematological diseases, the most common and most studied is cyclical neutropenia (CN) in which there is a periodic fall in the neutrophils from approximately normal to virtually zero and then back up again. This is typically accompanied by identical periodicities in the other granulocytic cells, red cell precursors, and platelets in both humans with CN and in the grey collie (the only known animal model for CN). In humans, these oscillations occur with a period ranging from 12 to 45 days (Haurie *et al.*, 1999a) while in the grey collie the period is between 12 and 15 days (Haurie *et al.*, 1999b). Treatment of CN with granulocyte colony stimulating factor (G-CSF) consistently decreases the period of the oscillation and increases both the mean value of the circulating neutrophils and the amplitude of their oscillation in both humans (Haurie *et al.*, 1999a) and the grey collie (Haurie *et al.*, 1999b).

There are aspects of the neutrophil dynamics in the grey collie that are puzzling, and these can be clearly seen in the serial neutrophil counts of nine untreated grey collies shown in Fig. 1.

‖ Author to whom correspondence should be addressed. 3655 Drummond Street, Room 1124, Montreal, Quebec, Canada H3G 1Y6. E-mail: mackey@cnd.mcgill.ca

0022–5193/00/120505 + 15 $35.00/0

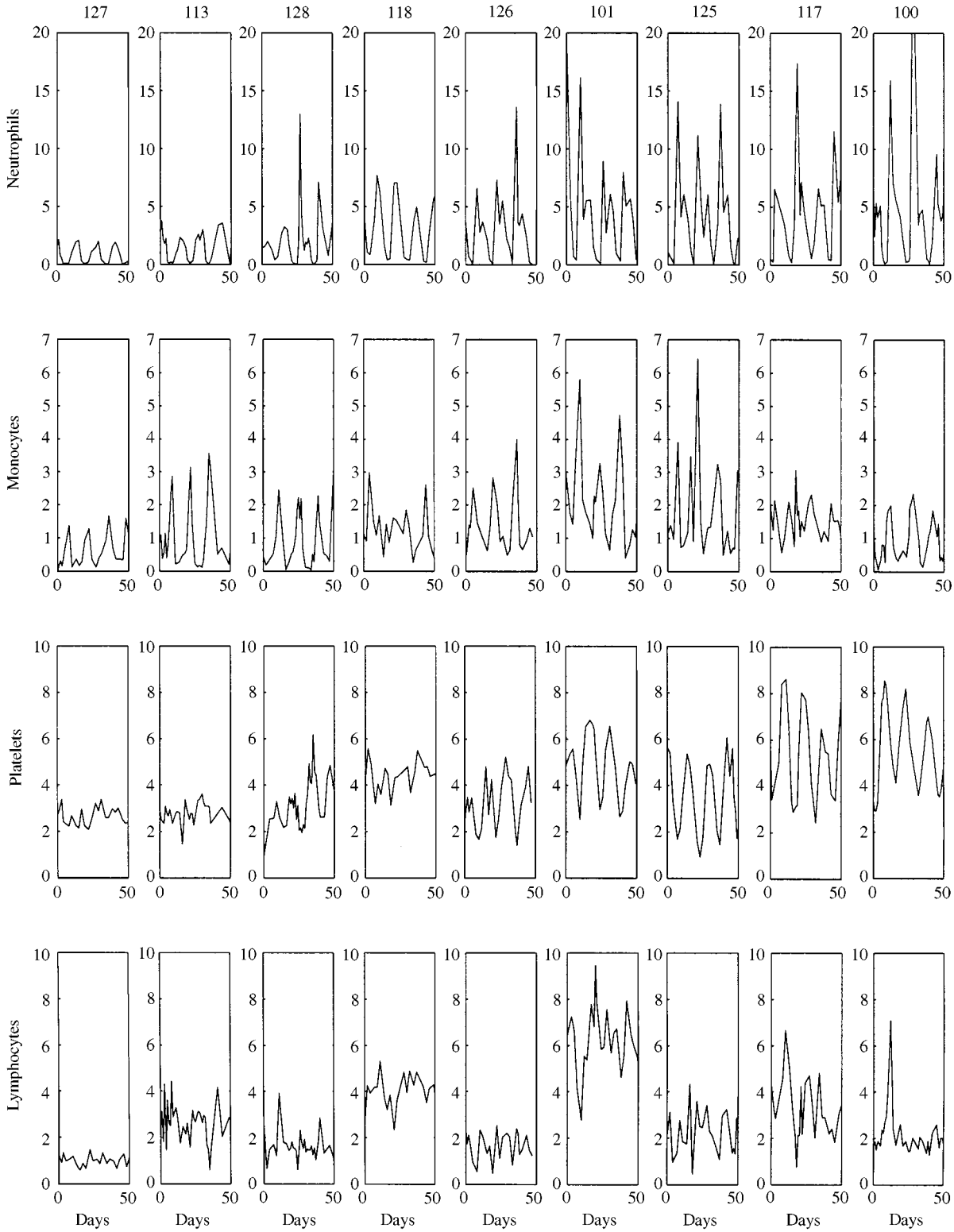

FIG. 1. Differential blood counts vs. time (in days) in nine grey collies. Units: cells $\times 10^{-5}$ mm^{-3} for the platelets and cells $\times 10^{-3}$ mm^{-3} for the other cell types. Redrawn from Haurie *et al.* (1999).

Firstly when the amplitude of the oscillation of the neutrophil count is low (e.g. Dog 127) the oscillation is approximately sinusoidal. However, as the amplitude increases, the form of the oscillation changes to one in which on the falling phase of the neutrophil counts there is a secondary transient "bump" or increase in the neutrophil count before the count finally falls to close to zero. This is especially evident to the eye for Dogs 126, 101, 125, 117, and 100. Secondly, the amplitude of the oscillations in the platelet counts follows the same general trend as for the neutrophils and the monocytes. Indeed, there is a positive relation between both the mean values and the amplitude of the oscillations in the neutrophil and platelet counts.

To further characterize the data in Fig. 1, we used the Lomb periodogram to detect periodicity in the blood cell counts (Lomb, 1976). This particular periodogram is tailored for unevenly sampled data sets, and the statistical significance (p value) of any peak in the periodogram can be calculated (Scargle, 1982).

Specifically, let x_j be the circulating density of a particular type of cell as measured at times t_j, where $j = 1, \ldots, N$ and N is the number of data points. As usual, the mean and variance of the data values are given by

$$\bar{x} \equiv \frac{1}{N} \sum_{i=1}^{N} x_j, \quad \sigma^2 \equiv \frac{1}{N-1} \sum_{i=1}^{N} (x_i - \bar{x})^2. \quad (1)$$

Then the *Lomb normalized periodogram* $P(f)$ at a frequency f is defined by

$$P(f) \equiv \frac{1}{\sigma^2} \left\{ \frac{[\sum_{j=1}^{N} (x_j - \bar{x}) \cos 2\pi f(t_j - \tau)]^2}{\sum_{j=1}^{N} \cos^2 2\pi f(t_j - \tau)} + \frac{[\sum_{j=1}^{N} (x_j - \bar{x}) \cos 2\pi f(t_j - \tau)]^2}{\sum_{j=1}^{N} \cos^2 2\pi f(t_j - \tau)} \right\}, \quad (2)$$

where the constant τ is defined implicitly by

$$\tan(4\pi f\tau) = \frac{\sum_{j=1}^{N} \sin(4\pi f t_j)}{\sum_{j=1}^{N} \cos(4\pi f t_j)}. \quad (3)$$

The value of $P(f)$ indicates the likelihood of a periodicity at a frequency f in the data set. We implemented eqn (2) for a series of different frequencies f. A judgement must be made as to whether or not there is a frequency for which the power $P(f)$ is significantly high. The estimation of the significance level of $P(f)$ is straightforward as long as some rules are followed for the choice of the range and the number of periods that are scanned (Press *et al*., 1992; Scargle, 1982). We implemented an adaptation of the procedure proposed in Press *et al*. (1992) using Matlab.

The unusual characteristics of the data of Fig. 1 are reflected in the corresponding Lomb power spectra shown in Fig. 2. Namely, the appearance of a secondary peak on the falling phase of the neutrophil count is associated with a secondary peak in the power spectrum at a frequency twice ($2f$, second harmonic) the fundamental frequency (f), and sometimes a third peak at the third harmonic ($3f$). Dogs 100 and 101 are especially noteworthy in this respect since the power at both the fundamental frequency f and the second harmonic ($2f$) are significant. The peak in the power at the third harmonic ($3f$) is also quite clear though not statistically significant. These characteristics are mirrored in the monocyte counts, and it should be remembered that the monocytes are derived from the same committed stem cell as are the neutrophils.

Many models of neutrophil production incorporate a peripheral negative feedback loop (Blumenson, 1973, 1975; Fokas *et al*., 1991; Rubinow, 1969; Rubinow *et al*., 1971; Rubinow & Lebowitz, 1975; 1976a, b; Smeby & Benestad, 1980; Steinbach *et al*., 1980; Wheldon, 1975; Wichmann & Loffler, 1988), and an alteration of this peripheral control has been proposed as the origin of CN by several authors (Kazarinoff & van den Driessche, 1979; King-Smith & Morley, 1970; MacDonald, 1978; Morley *et al*., 1969; Morley & Stohlman, 1970; Morley, 1970, 1979; Reeve, 1973; Schmitz, 1988; Schmitz *et al*., 1993, 1994, 1995, 1990; Shvitra *et al*., 1983; von Schulthess & Mazer, 1982; Wichmann *et al*., 1988). However, recent modeling (Hearn *et al*., 1998) has shown that a destabilization of this feedback pathway cannot account for the onset of oscillations seen in CN, and concluded that CN was probably not solely due to an instability in the peripheral feedback loop. This conclusion is consistent with the majority of clinical evidence and its interpretation (Haurie *et al*., 1998)

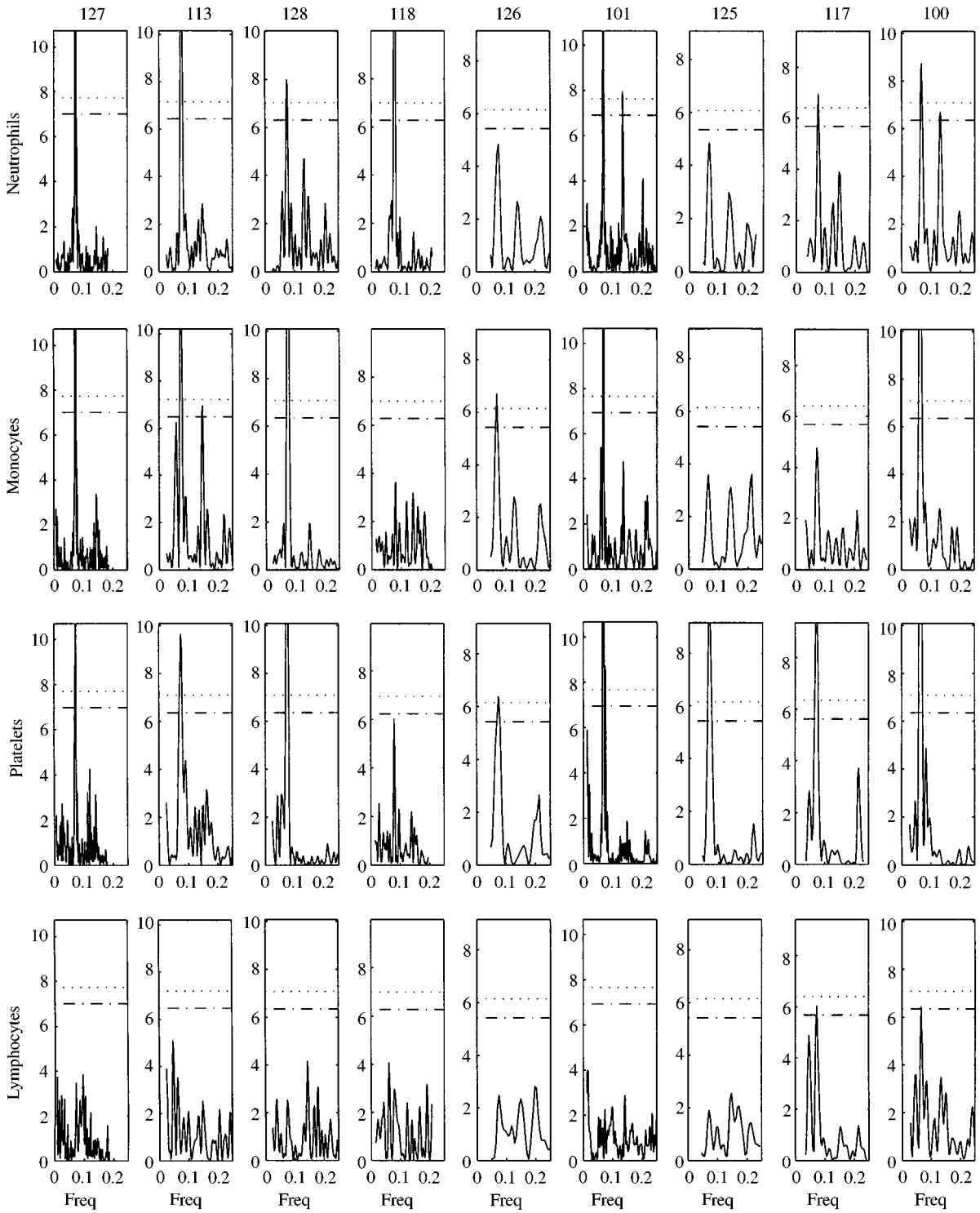

FIG. 2. Lomb periodogram $P(f)$ vs. frequency f of the differential blood counts in nine grey collies. The horizontal dotted line corresponds to a 0.05 significance level, while the dashed–dotted line is the 0.10 level. Redrawn from Haurie *et al.* (1999).

implicating the hematopoietic stem cell as the origin of the instability seen in CN.

In spite of the fact that a loss of stability in the peripheral control of neutrophil production does not seem to explain the origin of CN, the modeling of Hearn *et al.* (1998) can be used to understand the interesting neutrophil dynamics displayed in Figs 1 and 2. In this paper, we show

that the features of the neutrophil counts in grey collies and their power spectra are consistent with a nonlinear modification (by the peripheral control of neutrophil proliferation and maturation) of a periodic stem cell influx into the neutrophil differentiation pathway as suggested in Haurie *et al.* (1999).

Section 2 develops the specific version of the model of Hearn *et al.* (1998) that we use in this paper. The model differs from that of (Hearn *et al.* (1998) in that we explicitly include the modulation of apoptosis mediated by endogenous G-CSF in the control mechanisms. In Section 3, we analyse our model, showing in Section 3.1 conditions for which the steady state is globally stable. The near steady-state response of the model to a periodic forcing from the hematopoietic stem cell compartment is developed in Section 3.2 to give a theoretical basis for parameter estimation. There we show how the occurrence of higher-order harmonic components in the data may be understood. Section 4 deals with an estimation of the parameters of the model from the time-series data, from other sources, and from the analysis of Section 3.2. Section 5 gives the results of our simulations starting from these initial parameter estimates, and shows that the association of the second peak in the data is consistent with an increase in the mean value of the stem cell input to the system. The paper concludes with a brief discussion in Section 6.

2. Model Development

Let the density of white blood cells in the circulation be $x(t)$ (units of cells mm^{-3} blood), α the random disappearance rate of circulating white blood cells (days^{-1}), and $\mathscr{M}_o$ the production rate (cells $\mathrm{mm}^{-3}\,\mathrm{day}^{-1}$) of white blood cell precursors in the bone marrow.

Hearn *et al.* (1998) assumed that the rate of change of the peripheral (circulating) white blood cell density is made up of a balance between the loss of white blood cells ($-\alpha x$) and their production $[\mathscr{M}_o(\tilde{x})]$, so

$$\frac{\mathrm{d}x}{\mathrm{d}t} = -\alpha x + \mathscr{M}_o(\tilde{x}), \tag{4}$$

wherein $\tilde{x}(t)$ is $x(t-T)$ weighted by a distribution of maturation delays. $\tilde{x}(t)$ is given explicitly by

$$\tilde{x}(t) = \int_{T_m}^{\infty} x(t-u)g(u)\,\mathrm{d}u \equiv \int_{-\infty}^{t-T_m} x(u)g(t-u)\,\mathrm{d}u. \tag{5}$$

T_m is the minimal maturation delay and $g(T)$ is the density of the distribution of maturation delays as specified below. Since $g(T)$ is a density,

$$\int_0^{\infty} g(u)\,\mathrm{d}u = 1. \tag{6}$$

To completely specify the semi-dynamical system described by eqns (4) and (5) we must additionally give an initial function

$$x(t') \equiv \varphi(t') \quad \text{for } t' \in (-\infty, 0). \tag{7}$$

In Hearn *et al.* (1998) it was shown that the density of the gamma distribution

$$g(T) = \begin{cases} 0, & T \leqslant T_m \\ \dfrac{a^{m+1}}{\Gamma(m+1)}(T-T_m)^m \mathrm{e}^{-a(T-T_m)}, & T_m < T \end{cases}, \tag{8}$$

with $a, m \geqslant 0$, was able to give an excellent fit to the existing data on neutrophil maturation times. The parameters m, a, and T_m in the density of the gamma distribution can be related to certain easily determined statistical quantities. Thus, the average of the *unshifted* density is given by

$$T_2 = \int_0^{\infty} T g(T)\,\mathrm{d}T = \frac{m+1}{a} \tag{9}$$

so the average maturation delay is

$$\langle T \rangle = T_m + T_2 = T_m + \frac{m+1}{a} \tag{10}$$

TABLE 1
Distribution of maturation time parameters deduced from published data on normal dogs and grey collies. See Hearn et al. (1998) *for details*

Condition	$\langle T \rangle$ (*d*)	σ^2 (d^2)	T_m(*d*)	a (d^{-1})	m	Reference
Normal dog	3.68	0.198	3.0	3.43	1.33	Deubelbeiss *et al.* (1975)
Grey collie apogee	3.21	0.042	2.6	14.52	7.86	Patt *et al.* (1973)
Grey collie nadir	3.42	0.157	2.6	5.22	3.28	Patt *et al.* (1973)

and the variance (denoted by σ^2) is

$$\sigma^2 = \frac{m+1}{a^2}. \tag{11}$$

Using eqns (9) and (11) the gamma distribution parameters m and a are

$$a = \frac{T_2}{\sigma^2} \tag{12}$$

and

$$m = \frac{T_2^2}{\sigma^2} - 1. \tag{13}$$

Table 1 gives the values of $\langle T \rangle$, σ^2, T_m, a, and m consistent with the available data on the maturation time of neutrophils in normal dogs and grey collies as obtained in Hearn *et al.* (1998).

To write out the explicit form for the output flux $\mathcal{M}_o(\tilde{x}, t)$, the following considerations are important. It is assumed that the maximal amplification A_m of cells entering the recognizable neutrophil precursor pool is modified by apoptosis at a rate γ that is under the control of the number of circulating neutrophils $\tilde{x}_T$ so $\gamma = \gamma(\tilde{x})$. The maximal amplification is thereby modified to become $A_m \exp(-\gamma(\tilde{x})T)$, and if the input flux into the recognizable compartment of neutrophil precursors is $\mathcal{M}_i(t)$ then the efflux corresponding to the cells with transit time T is

$$\mathcal{M}_o(\tilde{x}, T) = \mathcal{M}_i A_m \mathrm{e}^{-\gamma(\tilde{x})T}. \tag{14}$$

To take into account the distribution of transit times we must integrate over the entire range of available transit times to give the final form for $\mathcal{M}_o(\tilde{x})$:

$$\mathcal{M}_o(\tilde{x}) \equiv \int_{T_m}^{\infty} \mathcal{M}_o(\tilde{x}, T) g(T)\, \mathrm{d}T$$

$$= \mathcal{M}_i A_m \mathrm{e}^{-\gamma(\tilde{x})T_m} \left[\frac{a}{a+\gamma(\tilde{x})}\right]^{m+1}. \tag{15}$$

In keeping with the known inverse relation between apoptosis and the levels of circulating G-CSF (Koury, 1992; Park, 1996; Williams *et al.*, 1990; Williams & Smith, 1993) and the inverse relation between circulating G-CSF levels and the peripheral neutrophil count (Kearns *et al.*, 1993; Mempel *et al.*, 1991; Takatani *et al.*, 1996; Watari *et al.*, 1989), we have taken a form for γ given by

$$\gamma(\tilde{x}) = \gamma_m \frac{\tilde{x}}{\theta + \tilde{x}} \tag{16}$$

so $\mathcal{M}_o$ will be a monotone decreasing function of $\tilde{x}$. Thus, the control of neutrophil production has the characteristics of a negative feedback system with distributed delay. The constants γ_m (the maximum rate of apoptosis) and θ (the value of $\tilde{x}$ at which apoptosis reaches half maximal values) in eqn (16) will be estimated in Section 4.

3. Analysis

3.1. STEADY STATES

The equilibrium solution for the functional differential equations (4) and (5) occurs when

$$\frac{\mathrm{d}x}{\mathrm{d}t} = 0 = -\alpha x + \mathcal{M}_o(\tilde{x}) \tag{17}$$

so the steady state x_* is defined implicitly by the solution of the equation

$$\alpha x_* = \mathscr{M}_o(x_*) \equiv \mathscr{M}_{o*}. \tag{18}$$

Given the monotone decreasing nature of the negative feedback production rate $\mathscr{M}_o(\tilde{x})$ inferred from the biology, there can be but a single unique value for the steady-state white blood cell density x_*. The value of $\mathscr{M}_{o*} = \alpha x_*$ is equivalent to the granulocyte turnover rate (GTR).

Let $f(x) = \mathscr{M}_o(x)/\alpha$. Then x_* is the unique root of the equation $f(s) = s$ in the interval $[0, \infty)$. Let $f^2 = f \circ f$. Then x_* is also a root of the equation $f^2(s) = s$. Now we give a sufficient condition for the global asymptotic stability of eqn (1).

Theorem 3.1. *Suppose that $\mathscr{M}_o$ is a continuous and decreasing function. Assume that x_* is the unique root of the equation $f^2(s) = s$ in the interval $[0, \infty)$. Let $\varphi : (-\infty, 0] \to [0, \infty)$ be a bounded function and $x(t)$ be the solution of eqn (1) satisfying the initial condition $x(t) = \varphi(t)$ for $t \in (-\infty, 0]$. Then $x(t)$ converges to x_* as $t \to \infty$.*

The proof of Theorem 3.1 is given in the Appendix. If $|\mathscr{M}_o'| < \alpha$, then $|f'| < 1$ and x_* is the unique root of $f^2(s) = s$. However, if the function $\mathscr{M}_o$ is of the form (15) then both analytic and numerical results indicate that x_* is the unique root of $f^2(s) = s$ if and only if $|\mathscr{M}_o'| \leqslant \alpha$. Thus, a sufficient condition for the global stability of x_* is

$$|\mathscr{M}_{o*}'| \leqslant \alpha. \tag{19}$$

3.2. RESPONSE TO FORCING

To develop the theoretical background for preliminary parameter estimates, we consider the response of this system to a periodic cellular influx coming from the hematopoietic stem cell compartment when we are near to a steady state. Throughout this analysis, an important parameter that will appear is the *slope* of the production function $\mathscr{M}_o$ evaluated at the steady state, denoted by $\mathscr{M}_{o*}'$. Because of our arguments concerning the negative feedback nature of the peripheral control mechanisms acting on neutrophil production, we know that this slope must be non-positive (i.e. negative or zero).

To examine the response to a periodic input, we assume that the production of neutrophils can be written in the form

$$\mathscr{M}_o(\tilde{x}, t) = \mathscr{M}_i(t) A(\tilde{x}), \tag{20}$$

where $A(\tilde{x})$ is the amplification within the neutrophil precursor compartment, and

$$\mathscr{M}_i(t) = \mathscr{M}_{i*}[1 + \varepsilon I(\bar{\omega}) e^{i\bar{\omega}t}], \quad \varepsilon \in [0, 1] \tag{21}$$

is the assumed oscillating hematopoietic stem cell influx with mean value $\mathscr{M}_{i*}$, amplitude $\varepsilon \mathscr{M}_{i*} Re[I(\bar{\omega})]$, and period $2\pi/\bar{\omega}$. The term

$$I(\bar{\omega}) = \int_{T_m}^{\infty} e^{-i\bar{\omega}T} g(T)\, dT = \left(\frac{a}{i\bar{\omega} + a}\right)^{m+1} e^{-i\bar{\omega}T_m} \tag{22}$$

accounts for the distribution of maturation times.

With these assumptions, we can write out eqn (4) for small deviations of x from x_*. In the first approximation this gives

$$\frac{dx}{dt} \simeq -\alpha x + \mathscr{M}_{o*} + (\tilde{x} - x_*)\mathscr{M}_{o*}' + \varepsilon I(\bar{\omega}) e^{i\bar{\omega}t}[\mathscr{M}_{o*} + (\tilde{x} - x_*)\mathscr{M}_{o*}'], \tag{23}$$

wherein

$$\mathscr{M}_{o*} \equiv \mathscr{M}_o(\tilde{x} = x_*) \tag{24}$$

and

$$\mathscr{M}_{o*}' \equiv \left.\frac{\partial \mathscr{M}_o(\tilde{x})}{\partial \tilde{x}}\right|_{\tilde{x} = x_*}. \tag{25}$$

Utilizing eqn (18) and defining the deviation from equilibrium as $z(t) = x(t) - x_*$, we can rewrite eqn (23) in the form

$$\frac{dz}{dt} + \alpha z - \mathscr{M}_{o*}'\tilde{z} = \varepsilon I(\bar{\omega}) e^{i\bar{\omega}t}[\mathscr{M}_{o*} + \mathscr{M}_{o*}'\tilde{z}]. \tag{26}$$

To use the existence of the first-, second-, and sometimes third-harmonic components evident

in the Lomb periodograms of Fig. 2 and reflected in the fits of eqn (32), we assume that the deviation z of the circulating neutrophil numbers from their steady-state value can be expanded in the series representation

$$z(t) = \sum_{k=0}^{\infty} c_k(\bar{\omega}) e^{ik\bar{\omega}t}. \tag{27}$$

Substituting eqn (27) into eqn (26) and equating the coefficients of the terms $\exp(ik\bar{\omega}t)$ for $k = 0, 1, 2$ yields $c_0(\alpha - \mathscr{M}'_{o*}) = 0$ as expected, so $c_0 \equiv 0$,

$$c_1(\bar{\omega}) = \frac{\varepsilon \mathscr{M}_{o*} I(\bar{\omega})}{\alpha + i\bar{\omega} - \mathscr{M}'_{o*} I(\bar{\omega})}, \tag{28}$$

and

$$c_2(\bar{\omega}) = c_1(\bar{\omega}) \frac{\varepsilon \mathscr{M}'_{o*} [I(\bar{\omega})]^2}{\alpha + i2\bar{\omega} - \mathscr{M}'_{o*} I(2\bar{\omega})}. \tag{29}$$

In the general case, the relation is

$$c_{k+1}(\bar{\omega}) = c_k(\bar{\omega}) \frac{\varepsilon \mathscr{M}'_{o*} I(\bar{\omega}) I(k\bar{\omega})}{\alpha + ik\bar{\omega} - \mathscr{M}'_{o*} I(k\bar{\omega})}. \tag{30}$$

From the above considerations, in the neighborhood of the steady state we can write

$$\begin{aligned} x(t) &\simeq x_* + Re[z(t)] \\ &= x_* + Re\left(\sum_{k=0}^{\infty} c_k(\bar{\omega}) e^{ik\bar{\omega}t} \right). \end{aligned} \tag{31}$$

We took all of the ANC of the nine grey collie dogs (see Fig. 1) and did a least-squares fit of the data to the equation

$$\begin{aligned} x(t) &= a_0 + \sum_{k=1}^{3} a_k \cos(k\bar{\omega}t + p_k) \\ &= a_0 + \sum_{k=1}^{3} a_k Re(e^{ik\bar{\omega}t + p_k}). \end{aligned} \tag{32}$$

The values of the constants $\bar{\omega}$, a_0, a_1 and a_2 resulting from these determinations are given in Table 2. The value of a_0 gives the average value of the circulating neutrophil number over several cycles in a given dog.

TABLE 2

The results of fitting the ANC data for 9 grey collies to eqn (32). The periods are given in days, and the units of the coefficients a are 10^3 *cells mm*$^{-3}$ *blood, or* 10^3 *cells kg*$^{-1}$ *body weight. The average circulating neutrophil level in a normal dog is about* 7.5×10^8 *cells kg*$^{-1}$ (*Deubelbeiss et al.*, 1975)

Dog	$\bar{\omega}$	Period	a_0	a_1	a_2
127	0.465	13.5	1.06	0.99	0.09
113	0.470	13.4	1.80	1.47	0.70
128	0.464	13.5	2.44	2.15	1.54
118	0.500	12.6	2.89	2.69	0.58
126	0.463	13.6	3.01	2.70	1.67
101	0.426	14.7	4.49	2.94	2.12
125	0.421	14.9	4.49	3.80	3.08
117	0.438	14.3	5.79	5.05	3.60
100	0.418	15.0	6.26	6.04	5.95

If we write the coefficients $c_k(\bar{\omega}_k)$ in polar form

$$c_k(\bar{\omega}) = |c_k(\bar{\omega})| e^{i \arg(c_k(\bar{\omega}_k))} \tag{33}$$

then we can identify $a_0 = x_*$ and

$$a_k = |c_k(\bar{\omega})|, \quad k = 1, 2, \ldots. \tag{34}$$

4. Parameter Estimation

α: The easiest parameter to estimate is α. Labeled neutrophils disappear from the circulation with a half-life $t_{1/2}$ of about 7 hr in both normal dogs (Deubelbeiss *et al.*, 1975) and grey collies (Dale *et al.*, 1972) with a range of 6.7–7.6 hr. The decay coefficient α of eqn (4) is related to the $t_{1/2}$ by

$$\alpha = \frac{\ln 2}{t_{1/2}} \tag{35}$$

so $\alpha \in [2.18, 2.48]$ (days^{-1}). We will take $\alpha = 2.4$ days^{-1} corresponding to $t_{1/2} = 7$ hr^{-1}.

ε and $\mathscr{M}'_{o*}$: To obtain estimates of ε and $\mathscr{M}'_{o*}$, use eqns (28) and (29) in eqn (34) to give

$$a_1 = \left| \frac{\varepsilon \mathscr{M}_{o*} I(\bar{\omega})}{\alpha + i\bar{\omega} - \mathscr{M}'_{o*} I(\bar{\omega})} \right|, \tag{36}$$

TABLE 3

Derived first estimates of the parameter values for the 9 grey collies of this study as determined by the methods described in Section 4. The values of ε and $\mathscr{M}'_{o*}$ are the average of the values determined for each using the parameters of Table 1 for the grey collie apogee and nadir distributions. The units of $\mathscr{M}'_{o*}$, γ_*, and γ_m are days^{-1}, θ is 10^3 cells mm^{-3} or 10^8 cells kg^{-1} body weight, and γ'_* is (days 10^3 cells mm^{-3})$^{-1}$ or (days 10^8 cells kg^{-1} body weight)$^{-1}$

			$\Gamma = 8$				$\Gamma = 16$			
Dog	ε	$\mathscr{M}'_{o*}$	γ_*	γ'_*	γ_m	θ	γ_*	γ'_*	γ_m	θ
127	0.95	−0.20	0.65	0.02	0.68	0.04	0.87	0.024	0.90	0.03
113	0.85	−0.91	0.65	0.06	0.56	0.28	0.87	0.065	1.01	0.28
128	0.93	−1.09	0.65	0.057	0.56	0.51	0.87	0.057	1.01	0.51
118	0.93	−0.48	0.65	0.021	0.56	0.72	0.87	0.021	1.01	0.72
126	0.94	−1.00	0.65	0.042	0.56	0.78	0.87	0.043	1.01	0.78
101	0.75	−1.24	0.65	0.035	0.56	1.73	0.87	0.035	1.01	1.73
125	0.96	−1.15	0.65	0.033	0.56	1.73	0.87	0.033	1.01	1.73
117	0.95	−1.05	0.65	0.023	0.56	2.88	0.87	0.023	1.01	2.88
100	1.09	−1.20	0.65	0.025	0.56	3.37	0.87	0.025	1.01	3.37

and

$$a_2 = \left| \frac{\varepsilon \mathscr{M}_{o*} I(\bar{\omega})}{\alpha + \mathrm{i}\bar{\omega} - \mathscr{M}'_{o*} I(\bar{\omega})} \cdot \frac{\varepsilon \mathscr{M}'_{o*} [I(\bar{\omega})]^2}{\alpha + \mathrm{i}2\bar{\omega} - \mathscr{M}'_{o*} I(2\bar{\omega})} \right|. \tag{37}$$

All of the quantities in these two equations are known from previous estimates except for ε and $\mathscr{M}'_{o*}$, and the result of solving for these two unknowns are tabulated in Table 3.

Two points are noteworthy.

First, in every case our analysis indicates that the amplitude ε of the oscillatory input (relative to the steady-state influx $\mathscr{M}_{i*}$) is close to one (for dog 100 it is 1.09, which is impossible) indicating that, if the model is correct, the influx from the stem cell compartment always cycles with a minimum close to zero.

Secondly, in every case the values of $\mathscr{M}'_{o*}$ consistent with the data are well above the Hopf bifurcation values of $\mathscr{M}'_{Hopf} \simeq -2.47$ as calculated in Hearn *et al.* (1998). This indicates that the neutrophil control loop modeled in this paper would have a locally stable steady state in the absence of any periodic stem cell inputs. This is consistent with the notion that the peripheral control of neutrophil production is not the origin of CN, a conclusion reached in Hearn *et al.* (1998) and elsewhere (Haurie *et al.*, 1998) based on other evidence. This further supports the idea that the hematopoietic stem cell population may be the source of the oscillations seen in cyclical neutropenia.

γ_*: Finally, two further relations can be derived from the steady-state relation (18) that will be of use in estimating the parameters γ_m and θ. Namely, at the steady state we have more explicitly

$$\alpha x_* = \mathscr{M}_{o*} = \mathscr{M}_{i*} A_* = \mathscr{M}_{i*} A_m \mathrm{e}^{-\gamma_* T_m} \left(\frac{a}{a + \gamma_*} \right)^{m+1}, \tag{38}$$

where $\gamma_* \equiv \gamma(x_*)$. Recognize that eqn (38) can be rewritten in the form

$$\Gamma \equiv \frac{A_m}{A_*} = \mathrm{e}^{\gamma_* T_m} \left(\frac{a + \gamma_*}{a} \right)^{m+1}, \tag{39}$$

where A_* is the steady-state amplification. In humans and normal mice, it is estimated that Γ is of the order of 8–16 (Hearn *et al.*, 1998), so with these values we can determine γ_* since all of the other parameters are known and tabulated in Table 1.

Additionally, at the steady state we have

$$\mathscr{M}'_{o*} = -\gamma'_* \mathscr{M}_{o*}\left[T_m + \frac{m+1}{a+\gamma_*}\right]. \tag{40}$$

Given an estimate of the GTR, $\mathscr{M}_{o*} = \alpha x_*$, eqn (38) gives an estimate of the maximum steady state $GTR_{max} = \mathscr{M}_{i*}A_m$ since γ_*, a, m and T_m are all known. Thus, given an estimate of γ_*, eqn (40) gives a direct estimate of γ'_* and $\mathscr{M}'_{o*}$ has been estimated.

To see how this can be used to determine values of the parameters γ_m and θ in eqn (16), note that

$$\gamma'_* = \gamma_m \frac{\theta}{(\theta + x_*)^2} \tag{41}$$

so it is easy to derive

$$\gamma_m = \frac{\gamma_*^2}{\gamma_* - \gamma'_* x_*} \quad \text{and} \quad \theta = \frac{x_*^2 \gamma'_*}{\gamma_* - \gamma'_* x_*}. \tag{42}$$

The results of our preliminary parameter estimations for the grey collies is contained in Table 3 for $\Gamma = 8$ and 16.

5. Simulation Results

With the model development of Section 2 and the preliminary parameter estimations of Section 4, we are now in a position to see if the full nonlinear simulation of our model is capable of reproducing the behavior seen in the data of Figs 1 and 2.

The full model as developed above can be written in the form

$$\frac{dx}{dt} = -\alpha x + \mathscr{M}_i(t) A_m e^{-\gamma(\tilde{x})T_m}\left[\frac{a}{a+\gamma(\tilde{x})}\right]^{m+1}, \tag{43}$$

by combining eqns (4) and (15), with an assumed periodic input of the form

$$\mathscr{M}_i(t) = \mathscr{M}_{i*}\{1 + \varepsilon Re[I(\bar{\omega})e^{i\bar{\omega}t}]\},\ \varepsilon \in [0,1] \tag{44}$$

and $\tilde{x}$ defined by eqn (5), and $\gamma(\tilde{x})$ an $I(\bar{\omega})$ given by eqns (16) and (22), respectively. Combining eqns (43) and (44) we have

$$\frac{dx}{dt} = -\alpha x + \mathscr{M}_{i*}A_m e^{-\gamma(\tilde{x})T_m}\left[\frac{a}{a+\gamma(\tilde{x})}\right]^{m+1} \times \{1 + \varepsilon Re[I(\bar{\omega})e^{i\bar{\omega}t}]\}. \tag{45}$$

The parameter α is known from the previous section, while a, T_m, and m are given in Table 1. From eqn (38), and remembering that $x_* = a_0$ from the previous section, we can write

$$\mathscr{M}_{i*}A_m = \alpha a_0 e^{\gamma_* T_m}\left(\frac{a+\gamma_*}{a}\right)^{m+1} \tag{46}$$

so given an estimate of γ_* we have an estimate of the coefficient $\mathscr{M}_{i*}A_m$. Further, given an estimate of $\mathscr{M}'_{o*}$ along with γ_* we can immediately estimate γ_m and θ.

We have simulated the solution behavior of the full model using xpp4w95, written by Prof. Bard Ermentrout. This freeware, for either Unix or Windows, is available at http://www.pitt.edu/~phase/. Selecting values of $\mathscr{M}'_{o*}$ and γ_*, we found that we were able to get the closest fit (as determined by visual examination) of the nine data sets using the final parameter values of Table 4, and the results of our numerical simulations are shown in Fig. 3. In every case, in order to mimic the approach of the ANC numbers to zero at the nadir of each oscillation it was necessary to take $\varepsilon = 1$. Comparison of the data of Fig. 1 and the Lomb analysis of Fig. 2 with the simulations of Fig. 3 indicates that there is a close correspondence.

6. Discussion

The simulations shown in Fig. 3, using parameters appropriate for the apogee distributions of maturation times as given in Table 1, are in good agreement with the data of Fig. 1 and with the spectral behavior shown in Fig. 2. When we used values of a and m derived from the nadir distributions, we found no appreciable change in the parameter values giving a good fit. Thus, from these model simulations we conclude that

TABLE 4

Parameter values for the 9 grey collies of this study that were used to produce the simulation results of Fig. 3. $\varepsilon \equiv 1$ *in every case, a, m, and* T_m *were taken from the apogee values of Table 1, and* $\bar{\omega}$ *was taken from the determinations of Table 2. Once* $\mathscr{M}'_{o*}$ *and* γ_* *are determined, the values of* γ'_*, γ_m, *and* θ, *given in the next three columns, are determined by eqns (40) and (42). In the last two columns,* Γ *is computed from eqn (39) and* $\mathscr{M}_{i*}A_m$ *(which is the maximal GTR) comes from eqn (46). The units of* $\mathscr{M}'_{o*}$, γ_*, *and* γ_m *are days*$^{-1}$, θ *is* 10^3 *cells mm*$^{-3}$ *or* 10^8 *cells kg*$^{-1}$ *body weight,* γ'_* *is (days* 10^3 *cells mm*$^{-3}$*)*$^{-1}$ *or (days* 10^8 *cell kg*$^{-1}$ *body weight)*$^{-1}$, *and* $\mathscr{M}_{i*}A_m$ *is* 10^3 *cells mm*$^{-3}$ *day*$^{-1}$ *or* 10^8 *cells kg*$^{-3}$ *body weight day*$^{-1}$

	From data fit		Eqns (40) and (42)			Eqns (39) and (46)	
Dog	$\mathscr{M}'_{o*}$	γ_*	γ'_*	γ_m	θ	Γ	$\mathscr{M}_{i*}A_m$
127	−0.10	0.20	0.0120	0.2136	0.071	1.90	4.95
113	−0.05	0.20	0.0035	0.2066	0.0590	1.90	8.41
128	−2.00	0.50	0.1045	1.0199	2.5370	4.95	29.73
118	−0.50	0.10	0.0219	0.2732	5.0055	1.38	9.80
126	−1.80	0.25	0.0760	2.9299	32.2660	2.23	16.50
101	−1.50	0.40	0.0437	0.7652	3.9903	3.60	38.69
125	−2.20	0.30	0.0623	4.4248	61.7350	2.62	28.88
117	−1.70	0.25	0.0373	1.8363	36.7390	2.23	31.74
100	−1.80	0.25	0.0365	2.9299	67.1047	2.23	34.32

the grey collie data are consistent with the hypothesis that there is a periodic influx of cells from the stem cell compartment. Further, since the model gives a reasonable representation of the secondary peak on the descending limb of the neutrophil counts we conclude that this phenomenon is simply due to the nonlinear filtering of a periodic stem cell input by the peripheral neutrophil control system mediated by G-CSF.

It is very important to note that the estimates of $\mathscr{M}'_{o*}$ all satisfy the global stability condition of $|\mathscr{M}'_{o*}| \leqslant \alpha$ as given in eqn (19). This supports the notion that the origin of the dynamic instability characterizing CN is not in the peripheral control of neutrophil production, and lends further weight to the central hypothesis of this paper. Namely, CN is due to a dynamic instability at the stem cell level.

Though the preliminary estimates of $\mathscr{M}'_{o*}$ in Table 3 are not too different from the final values of Table 4, there is quite a difference between the other preliminary parameter estimates and the actual values that were arrived at in the fit. The origin of this discrepancy is primarily due to the fact that the actual value of Γ as given in Table 4 ranges from about 2 to 5, values well below the previously estimated values of 8–16. Though we have no data that would allow us to estimate the value of Γ in normal dogs, if they have hematopoietic systems similar to humans and the mouse, the low values of Γ calculated here would suggest that the grey collie has much less "elasticity" available in their neutrophil control system to respond to increased demands for neutrophils. This decreased elasticity in the grey collie translates to between two and three fewer potential divisions within the neutrophil production system.

In the normal dog, the steady-state neutrophil production rate (GTR) is about 16.5×10^8 cells kg^{-1} day (Hearn *et al.*, 1998). If indeed, $8 < \Gamma < 16$ normally, then we should expect that the *maximal* normal GTR values are given by $132 \times 10^8 < \mathscr{M}_{i*}A_m < 264 \times 10^8$ cells kg^{-1} day. The maximal grey collie GTR values of $\mathscr{M}_{i*}A_m$ tabulated in Table 4 are much less than one-quarter of the minimum of this range. This suggests that in the grey collie there is not only an alteration within the stem cell compartment giving rise to the oscillatory dynamics, but that there is also a significant depression of the efflux from the stem cell population into the recognizable

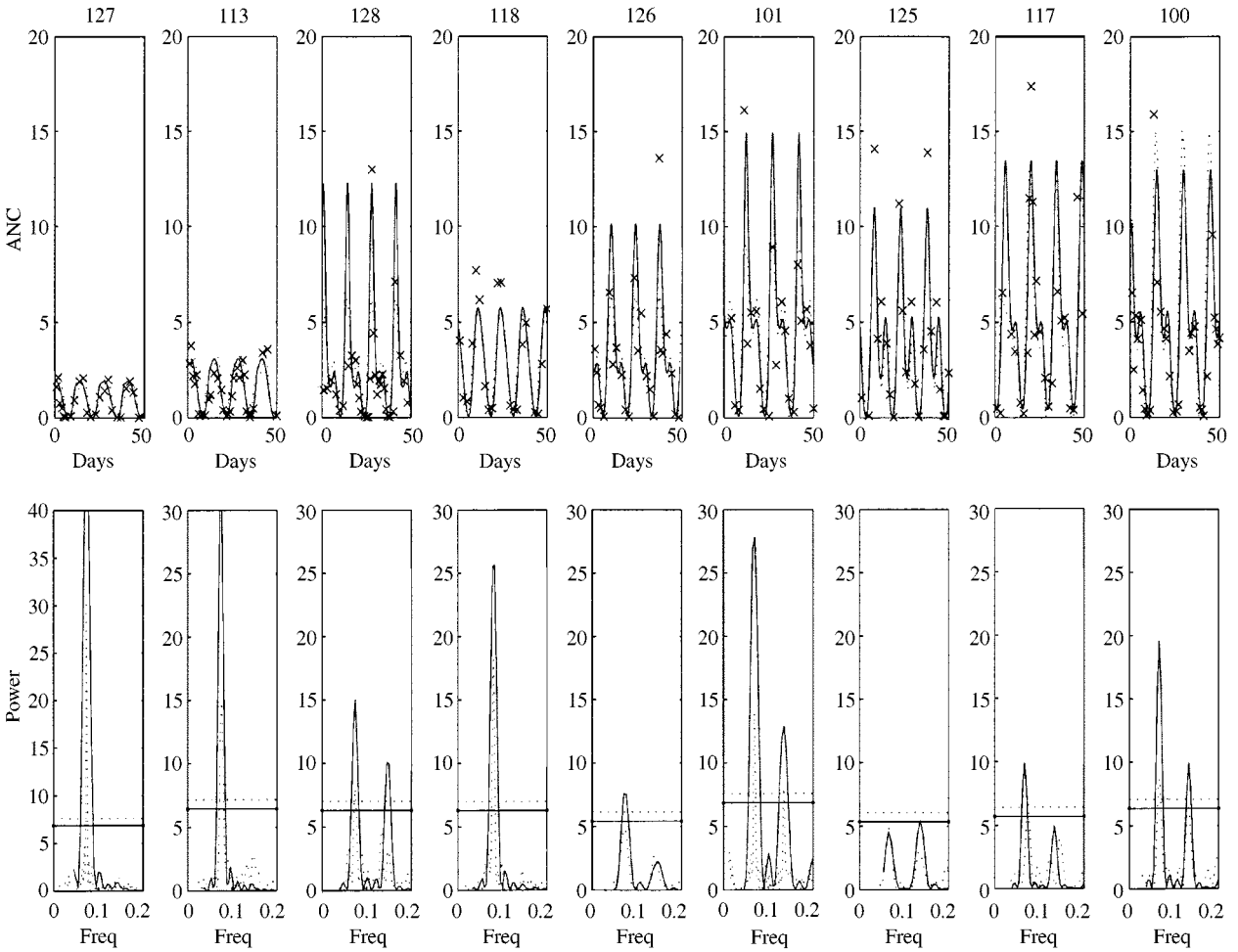

FIG. 3. Simulation results of fit of the model to the absolute neutrophil counts (ANC, top) and the Lomb periodogram of the ANC (bottom) in the nine grey collies. The units are as in Fig. 1. In the top panels, the x's are the data points, the dotted points correspond to the fit of the data to eqn (32), and the solid lines are the simulation results using the parameters of Table 4. In the bottom panel of nine figures, the dotted lines indicates the Lomb periodogram calculated for the best fit of the data by eqn (32), and the solid lines are the computed Lomb periodograms for the simulation results of the top panels.

neutrophil line. Taken together with the low values of Γ, we tentatively conclude that cyclical neutropenia is a hematopoietic defect in which there is abnormal cell loss within the stem cell compartment that is also expressed in the progeny committed to the production of neutrophils.

This same point has been emphasized experimentally by Avalos *et al.* (1994), who showed that normal dogs and grey collies had the same number of G-CSF receptors on neutrophil precursors, and that the binding constant of G-CSF with the receptor was unaltered between the two. They further found that grey collies required a sevenfold higher concentration of G-CSF to achieve half maximal colony growth compared to normal dogs, and concluded that the defect in cyclical neutropenia is "… due to a defect in the signal transduction pathway distal to G-CSF receptor binding …". Within the context of the model that we have presented and analysed, we provisionally interpret this experimental finding to imply that the values of γ_m tabulated in Table 4 are of the order of seven times the values that will be found in normal dogs. If this is correct, then we would expect that normally γ_m is between about 0.03 and 0.63 day^{-1}. Confirmation of this estimate must await further experimental work.

This work was supported by the Natural Sciences and Engineering Research Council (NSERC grant OGP-0036920, Canada), the Alexander von Humboldt Stiftung, Le Fonds pour la Formation de Chercheurs et l'Aide à la Recherche (FCAR grant 98ER1057, Québec), the National Institutes of Health (NIH Grant No. 18951, U.S.A.), the State Committee for Scientific Research (Poland) Grant No. 2 P03A 042 09, and the École Normale Supérieure de Paris. We thank Prof. Bard Ermentrout, University of Pittsburgh, author of xpp4w95, for his help. MCM would like to thank Prof. Erik Mosekilde of the Department of Physics, Technical University of Denmark, Lyngby, and Prof. Helmut Schwegler, Institute of Physics, Universität Bremen, Germany for their hospitality and support during the time some of this work was completed.

REFERENCES

AVALOS, B. R., BROUDY, V. C., CESELSKI, S. K., DRUKER, B. J., GRIFFIN, J. D. & HAMMOND, W. P. (1994). Abnormal response to granulocyte colony stimulating factor (G-CSF) in canine cyclic hematopoiesis is not caused by altered G-CSF receptor expression. *Blood* **84,** 789–794.

BLUMENSON, L. E. (1973). A comprehensive modeling procedure for the human granulopoietic system: over-all view and summary of data. *Blood* **42,** 303–313.

BLUMENSON, L. E. (1975). A comprehensive modeling procedure for the human granulopoietic system: detailed description and application to cancer chemotherapy. *Math. Biosci.* **26,** 217–239.

DALE, D. C., WARD, S. B., KIMBALL, J. R. & WOLFF, S. M. (1972). Studies of neutrophil production and turnover in grey collie dogs with cyclic neutropenia. *J. Clin. Invest.* **51,** 2190–2196.

DEUBELBEISS, K. A., DANCEY, J. T., HARKER, L. A. & FINCH, C. A. (1975). Neutrophil kinetics in the dog. *J. Clin. Invest.* **55,** 833–839.

FOKAS, A. S., KELLER, J. B. & CLARKSON, B. D. (1991). Mathematical model of granul-cytopoiesis and chronic myelogenous leukemia. *Cancer Res.* **51,** 2084–2091.

HAURIE, C., DALE, D. C. & MACKEY, M. C. (1998). Cyclical neutropenia and other periodic hematological diseases: a review of mechanisms and mathematical models. *Blood* **92,** 2629–2640.

HAURIE, C., DALE, D. C. & MACKEY, M. C. (1999a). Occurrance of periodic oscillations in the differential blood counts of congenital, idiopathic and cyclical neutropenic patients before and during treatment with G-CSF. *Exper. Hematol.* **27,** 401–409.

HAURIE, C., PERSON, R., DALE, D. C. & MACKEY, M. C. (1999b). Haematopoietic dynamics in grey collies. *Exper. Hematol.* **27,** 1139–1148.

HEARN, T., HAURIE, C. & MACKEY, M. C. (1998). Cyclical neutropenia and the peripherial control of white blood cell production. *J. theor. Biol.* **192,** 167–181.

KAZARINOFF, N. D. & VAN DEN DRIESSCHE, P. (1979). Control of oscillations in hematopoiesis. *Science* **203,** 1348–1350.

KEARNS, C. M., WANG, W. C., STUTE, N., IHLE, J. N. & EVANS, W. E. (1993). Disposition of recombinant human granulocyte colony stimulating factor in children with severe chronic neutropenia. *J. Pediatr.* **123,** 471–479.

KING-SMITH, E. A. & MORLEY, A. (1970). Computer simulation of granulopoiesis: normal and impaired granulopoiesis. *Blood* **36,** 254–262.

KOURY, M. J. (1992). Programmed cell death (apoptosis) in hematopoiesis. *Exp. Hematol.* **20,** 391–394.

LOMB, N. R. (1976). Least-squares frequency analysis of unequally spaced data. *Astrophys. Space Sci.* **39,** 447–462.

MACDONALD, N. (1978). Cyclical neutropenia: models with two cell types and two time lags. In: *Biomathematics and Cell Kinetics.* (Valleron, A. J. & MacDonald, P. D. M., eds), pp. 287–295. Amsterdam: Elsevier/North-Holland.

MEMPEL, K., PIETSCH, T., MENZEL, T., ZEIDLER, C. & WELTE, K. (1991). Increased serum levels of granulocyte colony stimulating factor in patients with severe congenital neutropenia. *Blood* **77,** 1919–1922.

MORLEY, A. (1970). Periodic diseases, physiological rhythms and feedback control—a hypothesis. *Aust. Ann. Med.* **3,** 244–249.

MORLEY, A. (1979). Cyclic hemopoiesis and feedback control. *Blood Cells* **5,** 283–296.

MORELY, A., KING-SMITH, E. A. & STOHLMAN, F. (1969). The oscillatory nature of hemopoiesis. In: *Hemopoietic Cellular Proliferation* (Stohlman, F., ed.), pp. 3–14. New York: Grune & Stratton.

MORELY, A. & STOHLMAN, F. (1970). Cyclophosphamide induced cyclical neutropenia. *New Eng. J. Med.* **282,** 643–646.

PARK, J. R. (1996). Cytokine regulation of apoptosis in hematopoietic precursor cells. *Curr. Opin. Hematol.* **3,** 191–196.

PATT, H. M., LUND, J. E. & MALONEY, M. A. (1973). Cyclic hematopoiesis in grey collie dogs: a stem-cell problem. *Blood* **42,** 873–884.

PRESS, W. H., TEUKOLSKY, S. A., VETTERLING, W. T. & FLANNERY, B. P. (1992) *Numerical Recipes in C*, 2nd Edn. Cambridge: Cambridge University.

REEVE, J. (1973). An analogue model of granulopoiesis for the analysis of isotopic and other data obtained in the non-steady state. *Br. J. Haematol.* **25,** 15–32.

RUBINOW, S. I. (1969). A simple model of a steady state differentiating cell system. *J. Cell Biol.* **43,** 32–39.

RUBINOW, S. I. & LEBOWITZ, J. L. (1975). A mathematical model of neutrophil production and control in normal man. *J. Math. Biol.* **1,** 187–225.

RUBINOW, S. I. & LEBOWITZ, J. L. (1976a). A mathematical model of the acute myeloblastic leukemia. *Biophy. J.* **16,** 897–891.

RUBINOW, S. I. & LEBOWITZ, J. L. (1976b). A mathematical model of the chemotherapeutic treatment of acute myeloblastic leukemia. *Biophys. J.* **16,** 1257–1271.

RUBINOW, S. I., LEBOWITZ, J. L. & SAPSE, A. M. (1971). Parameterization of *in vivo* leukemia cell populations. *Biophys. J.* **11,** 175–188.

SCARGLE, J. D. (1982). Studies in astronomical time series analysis. II. Statistical aspects of spectral analysis of unevenly spaced data. *The Astrophys. J.* **263,** 835–853.

SCHMITZ, S. (1988). Ein mathematisches Modell der zyklischchen Haemopoese. Ph.D. Thesis, Universität Köln.

SCHMITZ, S., FRANKE, H., BRUSIS, J. & WICHMANN, H. E. (1993). Quantification of the cell kinetic effects of G-CSF using a model of human granulopoiesis. *Exp. Hematol.* **21,** 755–760.

SCHMITZ, S., FRANKE, H., LOEFFLER, M., WICHMANN, H. E. & DIEHL, V. (1994). Reduced variance of bone-marrow transit time of granulopoiesis: a possible pathomechanism of human cyclic neutropenia. *Cell Prolif.* **27,** 655–667.

SCHMITZ, S., FRANKE, H., WICHMANN, H. E. & DIEHL, V. (1995). The effect of continuous G-CSF application in human cyclic neutropenia: a model analysis. *Br. J. Haematol.* **90,** 41–47.

SCHMITZ, S., LOEFFLER, M., JONES, J. B., LANGE, R. D. & WICHMANN, H. E. (1990). Synchrony of bone marrow proliferation of maturation as the origin of cyclic haemopoiesis. *Cell Tissue Kinet.* **23,** 425–441.

SHVITRA, D., LAUGALYS, R. & KOLESOV, Y. S. (1983). Mathematical modeling of the production of white blood cells. In: *Mathematical Modeling in Immunology and Medicine* (Marchuk, G. & Belykh, L. N., eds), pp. 211–223. Amsterdam: North-Holland.

SMEBY, W. & BENESTAD, H. B. (1980). Simulation of murine granulopoiesis. *Blut* **41,** 47–60.

STEINBACH, K. H., RAFFLER, H., PABST, G. & FLIEDNER, T. M. (1980). A mathematical model of canine granulocytopoiesis. *J. Math. Biol.* **10,** 1–12.

TAKATANI, H., SODA, H., FUKUDA, M., WATANABE, M., KINOSHITA, A., NAKAMURA, T. & OKA, M. (1996). Levels of recombinant human granulocyte colony stimulating factor in serum are inversely correlated with circulating neutrophil counts. *Antimicrob. Agents Chemother.* **40,** 988–991.

VON SCHULTHESS, G. K. & MAZER, N. A. (1982). Cyclic neutropenia (CN): a clue to the control of granulopoiesis. *Blood* **59,** 27–37.

WATARI, K., ASANO, S., SHIRAFUJI, N., KODO, H., OZAWA, K., TAKAKU, F. & KAMACHI, S. (1989). Serum granulocyte colony stimulating factor levels in healthy volunteers and patients with various disorders as estimated by enzyme immunoassay. *Blood* **73,** 117–122.

WHELDON, T. E. (1975). Mathematical models of oscillatory blood cell production. *Math. Biosci.* **24,** 289–305.

WICHMANN, H. E., LOEFFLER, M. & SCHMITZ, S. (1988). A concept of hemopoietic regulation and its biomathematical realization. *Blood Cells* **14,** 411–429.

WICHMANN, H. E. & LOEFFLER, M. (1988). *Mathematical Modeling of Cell Proliferation: Stem Cell Regulation in Hemopoiesis.* Boca Raton, FL: CRC Press.

WILLIAMS, G. T., SMITH, C. A., SPOONCER, E., DEXTER, T. M. & TAYLOR, D. R. (1990). Haemopoietic colony stimulating factors promote cell survival by suppressing apoptosis. *Nature* **353,** 76–78.

WILLIAMS, G. T. & SMITH, C. A. (1993). Molecular regulation of apoptosis: genetic controls on cell death. *Cell* **74,** 777–779.

APPENDIX

Proof of Theorem 1

First, observe that any solution $x(t)$ of eqn (1) is a bounded and nonnegative function. Since $0 \leqslant \mathscr{M}_o(x) \leqslant \mathscr{M}_o(0)$, a solution $x(t)$ of eqn (1) satisfies the inequalities

$$-\alpha x(t) \leqslant x'(t) \leqslant -\alpha x(t) + \mathscr{M}_o(0) \quad \text{for } t \geqslant 0.$$

As $x(0) \geqslant 0$ from the first inequality it follows that $x(t) \geqslant 0$ and the second inequality implies that $x(t)$ is a bounded function. Now we check that if

$$0 \leqslant A \leqslant \liminf_{t\to\infty} x(t) \leqslant \limsup_{t\to\infty} x(t) \leqslant B < \infty \tag{A.1}$$

then

$$\frac{1}{\alpha}\mathscr{M}_o(B) \leqslant \liminf_{t\to\infty} x(t) \leqslant \limsup_{t\to\infty} x(t) \leqslant \frac{1}{\alpha}\mathscr{M}_o(A). \tag{A.2}$$

Fix $\varepsilon > 0$. Then there exists $t_0 > 0$ such that

$$A - \varepsilon \leqslant x(t) \leqslant B + \varepsilon \quad \text{for } t \geqslant t_0. \tag{A.3}$$

We have

$$\tilde{x}(t) = \int_{T_m}^{t-t_0} x(t-u)g(u)\,\mathrm{d}u + \int_{t-t_0}^{\infty} x(t-u)g(u)\,\mathrm{d}u$$

for $t \geqslant t_0 + T_m$. From eqn (49) it follows that

$$\tilde{x}(t) \leqslant (B+\varepsilon)\int_{T_m}^{t-t_0} g(u)\,\mathrm{d}u + \gamma\int_{t-t_0}^{\infty} g(u)\,\mathrm{d}u, \tag{A.4}$$

where $\gamma = \sup\{|x(t)| : t \in \mathbf{R}\}$. Since g is a density there exists $t_1 > t_0 + T_m$ such that $\int_{t-t_0}^{\infty} g(s)\,\mathrm{d}s \leqslant \varepsilon$ for $t \geqslant t_1$. Consequently,

$$\tilde{x}(t) \leqslant B + \varepsilon + \gamma\varepsilon \quad \text{for } t \geqslant t_1.$$

Since $\mathscr{M}_o$ is a decreasing function we have

$$\mathscr{M}_o(\tilde{x}(t)) \geqslant \mathscr{M}_o(B + \varepsilon + \gamma\varepsilon) \quad \text{for } t \geqslant t_1.$$

This leads to the following differential inequality:

$$x'(t) \geqslant -\alpha x(t) + \mathscr{M}_o(B + \varepsilon + \gamma\varepsilon) \quad \text{for } t \geqslant t_1.$$

Let $y(t)$ be the solution of the equation

$$y'(t) = -\alpha y(t) + \mathscr{M}_o(B + \varepsilon + \gamma\varepsilon) \tag{A.5}$$

with the initial condition $x(t_1) = y(t_1)$. Then $x(t) \geqslant y(t)$ for $t \geqslant t_1$. Since the constant solution $y_0 \equiv \mathscr{M}_o(B + \varepsilon + \gamma_\varepsilon)/\alpha$ of eqn (A.5) is asymptotically stable we have $\lim_{t\to\infty} y(t) = y_0$. The inequality $x(t) \geqslant y(t)$ implies that

$$\liminf_{t\to\infty} x(t) \geqslant \mathscr{M}_o(B + \varepsilon + \gamma\varepsilon)/\alpha. \qquad \text{(A.6)}$$

Let $\varepsilon \to 0$. Then from eqn (A.6) we get

$$\liminf_{t\to\infty} x(t) \geqslant \frac{1}{\alpha}\mathscr{M}_o(B).$$

In a similar way, we obtain

$$\limsup_{t\to\infty} x(t) \leqslant \frac{1}{\alpha}\mathscr{M}_o(A).$$

Since the solution $x(t)$ of eqn (1) is a bounded function there exist constant A and B such that $0 \leqslant A < x_* < B$ and $A \leqslant x(t) \leqslant B$ for all $t \in \mathbf{R}$. From eqns (A.1) and (A.2) it follows that:

$$f^{2n}(A) \leqslant \liminf_{t\to\infty} x(t) \leqslant \limsup_{t\to\infty} x(t) \leqslant f^{2n}(B) \quad \text{(A.7)}$$

for $n = 1, 2, \ldots$. Since f is a decreasing function, the function f^2 is increasing. The assumption that x_* is the unique fixed point of the function f^2 in the interval $[0, \infty)$ implies that

$$x < f^2(x) < x_* \quad \text{for } x < x_*$$

and

$$x_* < f^2(x) < x \quad \text{for } x > x_*.$$

Hence,

$$\lim_{n\to\infty} f^{2n}(A) = x_* \quad \text{and} \quad \lim_{n\to\infty} f^{2n}(B) = x_*$$

and we finally obtain that

$$\lim_{t\to\infty} x(t) = x_*,$$

which completes the proof.